

Kondo enabled transmutation between spinons and superconducting vortices: Origin of magnetic memory in $4Hb\text{-TaS}_2$

Shi-Zeng Lin 

Theoretical Division, T-4 and CNLS, *Los Alamos National Laboratory*, Los Alamos, New Mexico 87545, USA
and Center for Integrated Nanotechnologies (CINT), *Los Alamos National Laboratory*, Los Alamos, New Mexico 87545, USA

 (Received 14 October 2022; revised 5 April 2024; accepted 14 May 2024; published 3 June 2024)

Recent experiments [Persky *et al.*, *Nature (London)* **607**, 692 (2022)] demonstrate a magnetic memory effect in $4Hb\text{-TaS}_2$ above its superconducting transition temperature, where Abrikosov vortices are spontaneously generated by lowering the temperature at zero magnetic field after field training the normal state. Motivated by the experiment, we propose the chiral quantum spin liquid (QSL) stabilized in the constituent layers of $4Hb\text{-TaS}_2$ as a mechanism. We model $4Hb\text{-TaS}_2$ as coupled layers of the chiral QSL and the superconductor. Through the Kondo coupling between the localized moments and conduction electrons, there is mutual transmutation between spinons and vortices during the thermal-cycling process, which yields the magnetic memory effect observed in experiments. We also propose a mechanism to stabilize chiral and nematic superconductivity in $4Hb\text{-TaS}_2$ through the Kondo coupling of conduction electrons to the chiral QSL. Our picture suggests $4Hb\text{-TaS}_2$ as an exciting platform to explore the interplay between QSL and superconductivity through the Kondo effect.

DOI: [10.1103/PhysRevResearch.6.023224](https://doi.org/10.1103/PhysRevResearch.6.023224)

I. INTRODUCTION

Quantum spin liquid (QSL) is an exotic state of matter, where electron spin fractionalizes into more elementary degrees of freedom that interact through a dynamical gauge field [1–4]. The existence of QSL has been well established by the exactly solvable models. Nevertheless, unambiguous experimental identification of the QSL remains a huge challenge, despite the fact that many encouraging signs have been detected. The QSL can serve as a mother state to induce other novel quantum states. For instance, one can obtain unconventional superconductivity by doping QSL [5] or by coupling QSL to metals through the Kondo coupling [6].

Recent observations of magnetic memory and spontaneous vortices in a van der Waals superconductor $4Hb\text{-TaS}_2$ suggest the possible existence of QSL in this compound [7]. $4Hb\text{-TaS}_2$ consists of two alternately stacked layers of octahedral TaS_2 ($1T\text{-TaS}_2$) and trigonal prismatic TaS_2 ($1H\text{-TaS}_2$). Both $1T\text{-TaS}_2$ and $1H\text{-TaS}_2$ can exist in a bulk form. The $1T\text{-TaS}_2$ bulk was argued to host QSL [8]. The $1T\text{-TaS}_2$ undergoes an incommensurate charge density wave (CDW) transition around 350 K, followed by another transition to a commensurate CDW around 200 K, forming a $\sqrt{13}\times\sqrt{13}$ structure [9]. The unit cell is enlarged to have 13 Ta ions, where each Ta ion contributes one $5d$ electron. The unit cell forms a triangular lattice. The observed insulating behavior implies a Mott-insulating state in $1T\text{-TaS}_2$ below 200 K. Indeed, the lower and upper Hubbard bands have been observed by a

scanning tunneling microscope [10,11]. However, no magnetic order and even the formation of the localized moment have been observed down to the lowest temperature, which is much lower than the estimated exchange coupling between localized spins [12–15]. These experiments support the existence of a QSL, either a fully gapped Z_2 QSL or a Dirac QSL, in $1T\text{-TaS}_2$ proposed by Law and Lee [8]. Later, more refined modeling calculations based on a spin Hamiltonian that is appropriate for $1T\text{-TaS}_2$ conclude a QSL with spinon Fermi surface [16]. The QSL picture is also supported by other measurements [11,17,18].

On the other hand, $2H\text{-TaS}_2$ (two layers of $1H\text{-TaS}_2$) is a superconductor with $T_c = 0.7$ K [19]. Therefore $4Hb\text{-TaS}_2$ offers an exciting platform for studying the interplay between superconductivity and QSL. One expects a Kondo coupling between the metallic layer $1H\text{-TaS}_2$ and the Mott insulator $1T\text{-TaS}_2$, which has been confirmed through the observation of the Kondo resonance peak by scanning tunneling microscopy [11,18,20]. Several unusual superconducting behaviors in $4Hb\text{-TaS}_2$, which may have the origin from this interplay, are observed in experiments. The T_c in $4Hb\text{-TaS}_2$ increases to 2.7 K. The two-dimensional nature of the superconducting state is confirmed by the extracted coherence lengths from the upper critical fields. Time-reversal symmetry (TRS) is found to be broken in the superconducting state from muon spin relaxation measurement and is interpreted as a signature for chiral superconductivity. Both the $d + id$ and $p + ip$ pairing symmetries that are constrained by the D_{3h} crystal structure are proposed [21]. The two-component superconducting order parameter is further supported by the Little-Parks oscillation and scanning tunneling microscopy and angle-resolved transport experiments [22]. Furthermore, a crossover from the chiral to the nematic state is also detected [23].

Published by the American Physical Society under the terms of the [Creative Commons Attribution 4.0 International](https://creativecommons.org/licenses/by/4.0/) license. Further distribution of this work must maintain attribution to the author(s) and the published article's title, journal citation, and DOI.

Recent experiments report an unusual magnetic memory effect in $4Hb$ -TaS₂ single crystals between $T_c = 2.7$ K and $T_M = 3.6$ K [7]. Initially, the crystal is cooled below $T = 1.7$ K below T_c in a small field $H = 1.3$ Oe to create a bunch of randomly distributed vortices due to the pinning potential. Then the crystal is warmed to $T_f > T_c$ under the same field, after which the crystal is zero-field cooled to a target temperature $T < T_c$. Surprisingly, there are randomly distributed vortices despite zero-field cooling. In experiments, this protocol is repeated, but at different T_f . The density of the remnant vortices decreases with T_f and disappears when $T_f > T_M$. The remnant vortex density increases linearly with the training magnetic field, and there exists a weak hysteresis near the zero field. The authors of Ref. [7] also performed annealing from $T > T_M$ to T_f with $T_c < T_f < T_Q$ in the training field. Then the crystal was cooled to $T < T_c$ without a magnetic field. In this process, no field is applied inside the superconducting phase. However, remnant vortices are observed, which is in sharp contrast to the case with zero-field cooling directly from $T > T_M$. The experiments point to an anomalous magnetic memory in $T_c < T < T_M$. In this temperature window, a small magnetization corresponding to one spin in an area of $40 \text{ nm} \times 40 \text{ nm}$ assuming a uniform distribution is observed. This small magnetization is not enough to induce the observed vortex density either due to Zeeman or orbital coupling to the conduction electrons. The authors of Ref. [7] speculate on the possibility of QSL with breaking TRS residing in the constituting $1T$ -TaS₂ layers as the origin of the memory effect, without knowing the underlying mechanism. Recently, a Z_2 QSL with TRS was proposed to explain the magnetic memory effect, where Z_2 vortices or visons are transformed into superconducting vortices at $T < T_c$ upon cooling [24]. A different mechanism based on magnetization amplification due to the interlayer pairing was discussed in Ref. [25]. A scenario based on the possibility of vortices in the Kondo coherence order parameter was also proposed [26].

II. MODEL

Our starting point is based on the experimental observation of the Kondo resonance peak in the bilayer of $1T$ -TaS₂/ $1H$ -TaS₂ [11,18]. The presence of a Kondo peak suggests negligible charge transfer between $1T$ -TaS₂ and $1H$ -TaS₂, and a well-developed localized magnetic moment in $1T$ -TaS₂ and the existence of itinerant electrons in $1H$ -TaS₂. Our physical picture is based on the understanding that, in the conventional heavy fermion liquid, the Kondo effect converts neutral spinons into charged fermions and, therefore, forms a heavy fermion liquid with an enlarged Fermi volume [27]. (The charge here is defined under the gauge fields of the electromagnetic fields.) We model $4Hb$ -TaS₂ as a superconductor–Mott insulator layered structure with an interlayer Kondo coupling (see Fig. 1). The Hamiltonian of $4Hb$ -TaS₂ can be schematically written as $\mathcal{H} = \mathcal{H}_T + \mathcal{H}_K + \mathcal{H}_H(c_i^\dagger, c_i)$, where \mathcal{H}_T [$\mathcal{H}_H(c_i^\dagger, c_i)$] describes $1T$ -TaS₂ ($1H$ -TaS₂), and \mathcal{H}_K is the Kondo interaction. They have the following forms (we set $\hbar = e = c = 1$ below):

$$\mathcal{H}_T = \sum_{(ij)} J_{ij} \mathbf{S}_i \cdot \mathbf{S}_j + \sum_{(ijkl)} J_{ijkl} (\mathbf{S}_i \cdot \mathbf{S}_j)(\mathbf{S}_k \cdot \mathbf{S}_l) + \dots, \quad (1)$$

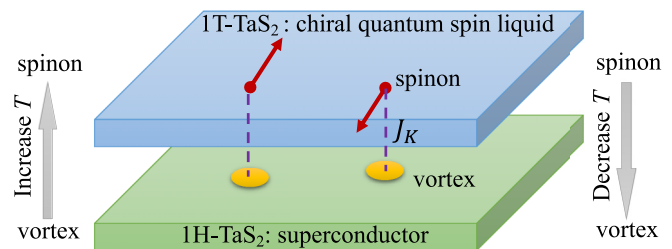


FIG. 1. $4Hb$ -TaS₂ is modeled as a multilayer structure with alternating chiral QSL and superconductor layers. Through the interlayer Kondo interaction, a superconducting vortex is dressed by a spinon. Transmutation between spinons and vortices occurs during the thermal-cycling process, which results in a magnetic memory effect in the temperature window $T_c < T < T_Q$.

$$\mathcal{H}_K = J_K \sum_i c_{i,\alpha}^\dagger \sigma_{\alpha\beta} c_{i\beta} \cdot \mathbf{S}_i. \quad (2)$$

$$\mathcal{H}_H = \sum_{i,j} t_{ij,\alpha\beta} c_{i,\alpha}^\dagger \sigma_{\alpha\beta} c_{j\beta} + \sum_k \Delta_k c_{k\uparrow}^\dagger c_{-k\downarrow}^\dagger + \text{H.c.} \quad (3)$$

We have included four spin interactions in \mathcal{H}_T and \dots represent higher-order interactions. The spin anisotropy in $1T$ -TaS₂ is small [16] and is neglected here. We use a general Hamiltonian \mathcal{H}_T with a superconducting order parameter $\Delta(k)$ to describe the electrons in $1H$ -TaS₂. The microscopic origin of the superconductivity and the pairing symmetry do not matter for the following discussion. Motivated by the experimental observation [7] of TRS breaking between T_c and T_m , and also the identification of chiral QSL [28] in the triangular lattice Hubbard model in the density matrix renormalization group study [29,30], here we assume that $1T$ -TaS₂ is in a chiral QSL below T_Q . The spin chirality $\mathbf{S}_i \cdot (\mathbf{S}_j \times \mathbf{S}_k)$ with ijk labeling the sites in the smallest triangle has a nonzero expectation value consistent with TRS breaking [31]. Denote $\chi \equiv \langle \mathbf{S}_i \cdot (\mathbf{S}_j \times \mathbf{S}_k) \rangle$, the mean-field Hamiltonian for \mathcal{H}_T in terms of \mathbf{S}_i becomes

$$\mathcal{H}_T = \tilde{J} \sum_{(ij)} \mathbf{S}_i \cdot \mathbf{S}_j + J_\chi \sum_{(ijk)} \mathbf{S}_i \cdot (\mathbf{S}_j \times \mathbf{S}_k), \quad (4)$$

where $J_\chi \propto \chi$, and \tilde{J} is the renormalized exchange coupling after the mean-field decoupling.

The chiral QSL and Kondo coupling can be treated using the parton construction, $\psi_i = (f_{i\uparrow}, f_{i\downarrow})^T$ with $\mathbf{S}_i = \sum_{\alpha\beta} f_{i\alpha}^\dagger \sigma_{\alpha\beta} f_{i\beta} / 2$ and $f_{i\uparrow}^\dagger f_{i\uparrow} + f_{i\downarrow}^\dagger f_{i\downarrow} = 1$. In the mean-field parton description,

$$\mathcal{H}_T \approx \sum_{ij} \psi_i^\dagger u_{i,j} \psi_j. \quad (5)$$

In this construction, \mathcal{H}_T has an SU(2) gauge redundancy [32] and $u_{i,j}$'s related by SU(2) gauge rotation are equivalent, i.e., $\psi_i \rightarrow W_i \psi_i$ and $u_{ij} \rightarrow W_i u_{ij} W_j^\dagger$, where W_i is a local SU(2) transformation [33]. We discuss two ansatzes. In the first case, the occupied $f_{i\alpha}$ forms a Chern band with Chern number $C = 1$, which can be obtained by introducing flux for $f_{i\alpha}$ hopping in the triangular lattice (see Fig. 2). The other ansatz corresponds to the state where $f_{i\alpha}$ is in the $d + id$ superconducting state [34].

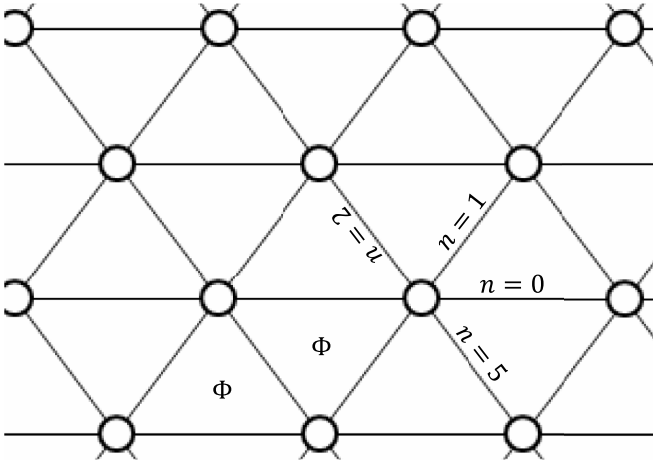


FIG. 2. Sketch of flux of the emergent gauge field \mathbf{a} in a triangular lattice. The spinons f_α hop in the background of \mathbf{a} flux and form Chern bands. All triangles have Φ flux.

The Kondo coherence can also be described in terms of the parton theory [27], where the Kondo term can be written as

$$\mathcal{H}_K = -J_K \sum_i (f_{i\alpha}^\dagger c_{i\alpha})(c_{i\beta}^\dagger f_{i\beta}) + \dots, \quad (6)$$

where we have neglected a shift in the local chemical potential for $c_{i\alpha}$ fermions. The Kondo coherence emerges when the composite bosons $f_{i\alpha}^\dagger c_{i\alpha}$ condense, $\langle f_{i\alpha}^\dagger c_{i\alpha} \rangle \neq 0$. Then the mean-field Hamiltonian for \mathcal{H}_K becomes

$$\mathcal{H}_K = -Q \sum_i (c_{i\beta}^\dagger f_{i\beta}) + \dots, \quad (7)$$

where $Q = J_K \langle f_{i\alpha}^\dagger c_{i\alpha} \rangle$. In the mean-field description, the total Hamiltonian is quadratic in f and can be solved. In the following, we assume a chiral QSL state, where the hopping phase in $u_{i,j}$ gives rise to a flux acting on the f fermions [34–36]. The strength of the flux should be determined self-consistently.

III. FIELD THEORY DESCRIPTION

In the presence of Kondo coherence, the $SU(2)$ gauge redundancy in ψ_i is Higgsed entirely. However, there exists remanent gauge redundancy associated with a simultaneous $U(1)$ rotation of f and c fermions. The f_α fermion carries a charge associated with an emergent gauge field \mathbf{a} , which is a subgroup of W_i . The c_α fermion carries a physical charge associated with the physical gauge field \mathbf{A} (actual electromagnetic fields). The condensation of Q locks \mathbf{A} to \mathbf{a} as a result of the Higgs mechanism. In the conventional heavy fermion liquid, the f_α fermions become part of the Fermi liquid of c_α , which enlarges the Fermi volume. We ascribe the observed memory effect in $4Hb$ -TaS₂ to a consequence of the coupling between \mathbf{A} and \mathbf{a} as detailed below.

The total Lagrangian of the system can be written as

$$\begin{aligned} \mathcal{L} = & \mathcal{L}_T(f_\sigma, \mathbf{a}) - \frac{\rho_Q}{2} [\nabla\theta - (\mathbf{a} - \mathbf{A})]^2 \\ & - \frac{\rho_\Delta}{2} (\nabla\phi - 2\mathbf{A})^2 + \dots, \end{aligned} \quad (8)$$

where we have neglected other terms for simplicity (i.e., quadratic and quartic terms in Q and Δ_k). We also neglected the fluctuations in the amplitude of Q and Δ_k , which are gapped in the ordered state. The kinetic terms describe the coupling between the phase fluctuation of $Q = |Q| \exp(i\theta)$ and $\Delta = |\Delta| \exp(i\phi)$ to the gauge fields, with ρ_Q and ρ_Δ being the phase stiffness. The superconducting order parameter Δ describes superconductivity in $1H$ -TaS₂, which can be intrinsic or induced by proximity to the chiral QSL. Δ Higgses \mathbf{A} , and the resulting theory has Z_2 -gauge symmetry. It is shown that doping chiral QSL can stabilize the chiral $d + id$ superconductivity [37,38]. One may also argue that similar superconductivity can emerge through the Kondo coupling. In our picture, only the Higgs mechanics, which is universal regardless of the pairing mechanism and symmetry, is important for the current discussion. \mathcal{L}_T describes the quantum state of $1T$ -TaS₂. In the chiral QSL, f_α forms a Chern insulator with the occupied up- and down-spin bands having a Chern number $C = 1$. We can integrate out the f_α , which results in the Chern-Simon Lagrangian

$$\mathcal{L}_T(f_\sigma, \mathbf{a}) = \frac{2C}{4\pi} \epsilon^{\mu\nu\rho} a_\mu \partial_\nu a_\rho - \mathbf{J}_f \cdot \mathbf{a}, \quad (9)$$

where we have included the probe charge \mathbf{J}_f . The ground state described by \mathcal{L}_T is doubly degenerate and supports excitation spinons as semions. Each spinon f_α carries the π/C flux of \mathbf{a} , which can be seen by varying \mathcal{L}_T with respect to a_0 . This flux attachment is also responsible for the semion statistics of f_α .

With Kondo coherence, the emergent flux in \mathbf{a} becomes the physical magnetic flux in \mathbf{A} due to the Higgs mechanism. To describe $4Hb$ -TaS₂, we assume that the field strength of \mathbf{a} is weak, such that in the Meissner phase it is fully expelled from the sample where the superconducting and Kondo coherence coexist.

The physics depends on three temperatures, T_c , T_Q , and the Kondo coherence temperature T_K . In the experimentally relevant case $T_Q > T_c$, the magnetic memory exists (disappears) when $T_K > T_c$ ($T_K < T_c$). Experimentally $T_K \approx 18$ K in the bilayer of $1T$ -TaS₂ and $1H$ -TaS₂ [11] and we focus on the case with $T_K > T_c$ and $T_K > T_Q$ in the following discussion. The transmutation between spinons and vortices depends on the phase stiffness ρ_Q and ρ_Δ . We assume that $\rho_Q \gg \rho_\Delta$, such that \mathbf{a} is always locked to \mathbf{A} . In the opposite limit, spinons induce vortices in Q instead [26].

Now we are in a position to interpret the magnetic memory effect during the thermal cycling of $4Hb$ -TaS₂ in the experiment. When the system is cooled below T_c under a weak magnetic field, a certain magnetic flux is trapped inside the system in the form of Abrikosov vortices and is pinned by defects. Each vortex carries π flux of \mathbf{A} . The Q condensate locks \mathbf{A} to \mathbf{a} and induces π flux in \mathbf{a} , which attaches one spinon to the vortex. Warming the system in the same field above T_c but below T_Q destroys vortices. Some of the spinons relax and become part of the Chern bands, while the other can be pinned by defects. When the system is zero-field cooled below T_c from this state, these trapped spinons induce vortices due to the Kondo effect. As the temperature for field training T_f increases toward T_Q , the pinning energy of spinons decreases. As a result, the residual field due to the vortices at the end of thermal cycling decreases with T_f . It is also clear that the

remnant field increases linearly with the density of the initial vortices, hence the training field as observed in experiment. Hysteresis naturally occurs due to the pinning of spinons and vortices. The diminishing of the hysteresis at a larger training field in the experiments may be due to the interaction between vortices.

The charge of spinon under \mathbf{a} carried by the π flux of \mathbf{a} depends on the sign of C and hence the sign of $\langle \mathbf{S}_i \cdot (\mathbf{S}_j \times \mathbf{S}_k) \rangle$. The π flux of \mathbf{a} corresponds to the positive-charged (negative-charged) spinon under \mathbf{a} for $C = 1$ ($C = -1$). The positive-charged (negative-charged) spinon corresponds to an excess (vacant) spinon in a magnetic unit cell of \mathbf{a} . In the mean-field description, the vacant spinons can be a localized spin, which does not fractionalize into spinons. An excess spinon corresponds to the case where the magnetic unit cell of \mathbf{a} is enlarged to contain three spin sites. In real systems, it is likely that there exist multiple domains of chiral QSL with different C similar to the Chern insulators [39,40]. In each domain, the charge of the induced spinons depends on C . Nevertheless, during the thermal-cycling process, the polarization of the vortices is the same as that of the original vortices regardless of the sign of C .

We then discuss the nucleation of Abrikosov vortices for the protocol when the training magnetic field is applied only between T_c and T_Q . Without the training field, it is natural to form chiral QSL mosaics with opposite C numbers. Within each domain, there exist regions with excess or vacant spinons. These chiral QSL mosaics with excess or vacant spinons tend to induce vortices and antivortices through the Kondo coupling. Well-separated vortices can form only when the separation of spinons and the size of the chiral QSL domain far exceed the size of vortices, which is of the order of the London penetration depth. The size of a vortex in $4Hb$ -TaS₂ is around 5 μm according to the experimental image of the vortex using the scanning superconducting quantum interference device [7]. It is likely that the vortex size is comparable to or even larger than the size of the chiral QSL domains. As an example, the size of Chern domains in the Chern insulator is smaller than 1 μm [40]. In this case, no vortices are generated during the cooling process without a training field. In the presence of a training field, one type of chiral domain is favored through the weak orbital coupling between the spin chirality $\mathbf{S}_i \cdot (\mathbf{S}_j \times \mathbf{S}_k)$ and the magnetic field [41–43]. As a result, the favored chiral domains grow in size, and the spinons can generate vortices when the domain sizes are larger than the vortex size. The training field also couples to the spinons through a direct Zeeman coupling, but this coupling does not select the polarization of the vortex. The position where the spinons or vortices get trapped depends on the pinning potential landscape of the system and also on the history of thermal cycling.

The physical picture presented here suggests the existence of *localized* spinons. The spinons in the normal state below T_Q generate a weak magnetization that is much smaller than the magnetization associated with vortices. A weak magnetization corresponding to one spin-1/2 moment in an area of 40 nm \times 40 nm on average is indeed observed in the experiment [7], which supports the current physical picture.

We proceed to discuss the other chiral QSL ansatz with f_α in the $d + i\eta d$ pairing state and its connection to the

unconventional superconducting properties of $4Hb$ -TaS₂ observed in experiment. The ansatz for this state can be written as

$$u_{\mathbf{r},\mathbf{r}+\mathbf{r}_n} = \lambda\tau_z + \gamma[\cos(n2\pi/3)\tau_x - \eta\tau_y \sin(n2\pi/3)], \quad (10)$$

where τ_μ are Pauli matrices acting in the spinor space of ψ_i , and $n = 0, 1, \dots, 5$ counterclockwise enumerates the bonds that connect to the site \mathbf{r} (see Fig. 2). We introduce the parameter η to characterize the ratio between the two d -wave components. For $\eta \neq 1$, the QSL ansatz breaks the C_3 rotation symmetry of $4Hb$ -TaS₂ even in the absence of Kondo coherence when there exists $SU(2)$ gauge redundancy, hence describing a nematic state. This can be seen by writing $u_{\mathbf{r},\mathbf{r}+\mathbf{r}_n} = \mathbf{d}_n \cdot \boldsymbol{\tau}$. $|d_n|$ is different for different bonds. $SU(2)$ gauge transformation preserves $|d_n|$ and therefore cannot restore the C_3 rotation symmetry. The chiral QSL with the $d + i\eta d$ ansatz has Z_2 -gauge symmetry and supports e , m , and ϵ anyons [44]. The m anyon is a vortex of the $d + i\eta d$ pairing state and carries the π flux of \mathbf{a} . The discussion of the transmutation between spinons and Abrikosov vortices for the Chern band ansatz can be extended straightforwardly to the chiral QSL with the $d + i\eta d$ ansatz, but with the replacement of spinons by m anyons. The $d + i\eta d$ ansatz is relevant here because it automatically engenders chiral superconductivity with $d + i\eta d$ pairing symmetry when Kondo coherence sets in. This provides a mechanism for the observed chiral and nematic superconductivity in $4Hb$ -TaS₂ with elevated T_c compared to the $2H$ -TaS₂ compound [21,23].

IV. DISCUSSION AND SUMMARY

The related idea of the transmutation between visons in Z_2 QSL and Abrikosov vortices was discussed in the context of cuprate superconductors [45]. There the pseudogap phase is identified as a Z_2 QSL, which can be accessed by raising the temperature from the d -wave superconducting state. In cylindrical geometry, a trapped magnetic flux in the superconducting state is transmuted to a Z_2 vison or vice versa during the thermal-cycling process. This was proposed as smoking-gun evidence for the existence of topological order in the pseudogap phase. This idea was adopted and extended by Chen [24] to explain the magnetic memory effect in $4Hb$ -TaS₂. The proposed Z_2 QSL preserves TRS, which contradicts the experimentally observed TRS breaking state above T_c . In experiments, when the system is cooled from the field-trained state above T_c , only vortices with polarization aligned with the training field are generated. Here, we assume a chiral QSL, and polarization of the magnetic field is memorized by the system through the Chern number of the spinon bands or sign of $\langle \mathbf{S}_i \cdot (\mathbf{S}_j \times \mathbf{S}_k) \rangle$. The polarization of the generated vortices is therefore determined by the training field, which is consistent with the experiments. Furthermore, the chiral QSL can also provide a mechanism for stabilizing chiral superconductivity in $4Hb$ -TaS₂.

We remark that the $U(1)$ QSL, where spinons form a neutral Fermi surface and are coupled to an emergent $U(1)$ gauge field, was proposed for $1T$ -TaS₂ [16,18]. The QSL can persist up to 200 K. It is possible that the coupling between $1T$ -TaS₂ and $1H$ -TaS₂ in $4Hb$ -TaS₂ modifies the magnetic interactions and stabilizes the chiral QSL below T_Q . There can

be a transition between the U(1) QSL and the chiral QSL. A finite-temperature transition of chiral QSL is allowed even in the two-dimensional limit because the QSL breaks the discrete Z_2 symmetry associated with $\mathbf{S}_i \cdot (\mathbf{S}_j \times \mathbf{S}_k)$. The chiral QSL in the Mott insulator generates quantized thermal Hall conductance. In the metallic $4Hb$ -TaS₂, there can exist a chiral metallic state in the temperature region $T_c < T < T_Q, T_K$, which can be verified by thermal or electrical Hall conductance measurement. This chiral metallic state may also be absent when superconductivity is induced by the Kondo coupling to the chiral QSL with the $d + i\eta d$ ansatz, such that $T_c = T_K$. Whether the superconductivity is induced by the chiral QSL or other bosonic fluctuations can be distinguished by measuring the split of the transition temperature under strain. When the D_{3h} crystal symmetry is reduced by strain, the transition temperature for the two-component order parameters splits for the bosonic-fluctuation-mediated superconductivity. In contrast, for chiral QSL-induced chiral superconductivity, there is no split of the transition temperature.

The composite spinon-vortex object can be detected by scanning tunneling microscopy (STM) measurement. Below T_c , one can visualize the superconducting vortex by measuring the local tunneling conductivity by STM. At $T_c < T < T_Q$, the vortex disappears, while the spinon component remains. Because of a finite charge gap, which is of the order of the Coulomb interaction, the charge degree of freedom is not frozen completely. It is demonstrated theoretically that the spinon carries a physical electric charge due to fluctuations of the remnant charge [36], which can be measured by STM.

It is known that the Kondo effect connects the QSLs to their charged partners through the Higgs mechanism associated

with the Kondo coherence [27,46]. As a concrete example, here we demonstrate the transmutation of neutral excitations to charged excitations under physical electromagnetic fields in the chiral QSL and superconductor heterostructures. This points to a promising route for experimental detection of neutral excitations in strongly correlated systems, which is at the heart of the controversy in modern condensed-matter physics. Therefore, the $1T$ -TaS₂ and $1H$ -TaS₂ heterostructures are a promising platform for demonstrating this physics by varying T_c, T_K , and T_Q in a controlled way.

In summary, we propose that the Kondo coupling between a chiral quantum spin liquid and a superconductor allows for transmutation between spinons and superconducting vortices. This results in a magnetic memory effect, which explains the same effect observed in $4Hb$ -TaS₂. Our results further support the existence of the chiral quantum spin liquid in $4Hb$ -TaS₂. We also suggest that the chiral quantum spin liquid may be responsible for the unconventional superconductivity in $4Hb$ -TaS₂.

ACKNOWLEDGMENTS

We acknowledge the helpful discussions with Qimiao Si and Elio König. The work at LANL was carried out under the auspices of the U.S. DOE NNSA under Contract No. 89233218CNA000001 through the LDRD Program and was performed, in part, at the Center for Integrated Nanotechnologies, an Office of Science User Facility operated for the U.S. DOE Office of Science, under User Proposals No. 2018BU0010 and No. 2018BU0083.

-
- [1] L. Balents, Spin liquids in frustrated magnets, *Nature (London)* **464**, 199 (2010).
- [2] L. Savary and L. Balents, Quantum spin liquids: A review, *Rep. Prog. Phys.* **80**, 016502 (2017).
- [3] Y. Zhou, K. Kanoda, and T.-K. Ng, Quantum spin liquid states, *Rev. Mod. Phys.* **89**, 025003 (2017).
- [4] H. Takagi, T. Takayama, G. Jackeli, G. Khaliullin, and S. E. Nagler, Concept and realization of Kitaev quantum spin liquids, *Nat. Rev. Phys.* **1**, 264 (2019).
- [5] P. Anderson, Resonating valence bonds: A new kind of insulator? *Mater. Res. Bull.* **8**, 153 (1973).
- [6] P. Coleman and N. Andrei, Kondo-stabilised spin liquids and heavy fermion superconductivity, *J. Phys.: Condens. Matter* **1**, 4057 (1989).
- [7] E. Persky, A. V. Bjørlig, I. Feldman, A. Almoalem, E. Altman, E. Berg, I. Kimchi, J. Ruhman, A. Kanigel, and B. Kalisky, Magnetic memory and spontaneous vortices in a van der Waals superconductor, *Nature (London)* **607**, 692 (2022).
- [8] K. T. Law and P. A. Lee, $1T$ -TaS₂ as a quantum spin liquid, *Proc. Natl. Acad. Sci. USA* **114**, 6996 (2017).
- [9] J. Wilson, F. Di Salvo, and S. Mahajan, Charge-density waves and superlattices in the metallic layered transition metal dichalcogenides, *Adv. Phys.* **24**, 117 (1975).
- [10] S. Qiao, X. Li, N. Wang, W. Ruan, C. Ye, P. Cai, Z. Hao, H. Yao, X. Chen, J. Wu, Y. Wang, and Z. Liu, Mottness collapse in $1T$ -TaS_{2-x}Se_x transition-metal dichalcogenide: An interplay between localized and itinerant orbitals, *Phys. Rev. X* **7**, 041054 (2017).
- [11] V. Vaňo, M. Amini, S. C. Ganguli, G. Chen, J. L. Lado, S. Kezilebieke, and P. Liljeroth, Artificial heavy fermions in a van der Waals heterostructure, *Nature (London)* **599**, 582 (2021).
- [12] A. Ribak, I. Silber, C. Baines, K. Chashka, Z. Salman, Y. Dagan, and A. Kanigel, Gapless excitations in the ground state of $1T$ -TaS₂, *Phys. Rev. B* **96**, 195131 (2017).
- [13] M. Klanjšek, A. Zorko, R. Žitko, J. Mravlje, Z. Jaglič, P. K. Biswas, P. Prelovšek, D. Mihailovic, and D. Aron, A high-temperature quantum spin liquid with polaron spins, *Nat. Phys.* **13**, 1130 (2017).
- [14] S. Mañas-Valero, B. M. Huddart, T. Lancaster, E. Coronado, and F. L. Pratt, Quantum phases and spin liquid properties of $1T$ -TaS₂, *npj Quantum Mater.* **6**, 69 (2021).
- [15] I. Benedičič, N. Janša, M. van Midden, P. Jeglič, M. Klanjšek, E. Zupanič, Z. Jagličič, P. Šutar, P. Prelovšek, D. Mihailovič, and D. Arčon, Superconductivity emerging upon Se doping of the quantum spin liquid $1T$ -TaS₂, *Phys. Rev. B* **102**, 054401 (2020).
- [16] W.-Y. He, X. Y. Xu, G. Chen, K. T. Law, and P. A. Lee, Spinon Fermi surface in a cluster Mott insulator model on a triangular lattice and possible application to $1T$ -TaS₂, *Phys. Rev. Lett.* **121**, 046401 (2018).

- [17] H. Murayama, Y. Sato, T. Taniguchi, R. Kurihara, X. Z. Xing, W. Huang, S. Kasahara, Y. Kasahara, I. Kimchi, M. Yoshida, Y. Iwasa, Y. Mizukami, T. Shibauchi, M. Konczykowski, and Y. Matsuda, Effect of quenched disorder on the quantum spin liquid state of the triangular-lattice antiferromagnet $1T$ -TaS₂, *Phys. Rev. Res.* **2**, 013099 (2020).
- [18] W. Ruan, Y. Chen, S. Tang, J. Hwang, H.-Z. Tsai, R. L. Lee, M. Wu, H. Ryu, S. Kahn, F. Liou, C. Jia, A. Aikawa, C. Hwang, F. Wang, Y. Choi, S. G. Louie, P. A. Lee, Z.-X. Shen, S.-K. Mo, and M. F. Crommie, Evidence for quantum spin liquid behaviour in single-layer $1T$ -TaSe₂ from scanning tunnelling microscopy, *Nat. Phys.* **17**, 1154 (2021).
- [19] S. Nagata, T. Aochi, T. Abe, S. Ebisu, T. Hagino, Y. Seki, and K. Tsutsumi, Superconductivity in the layered compound $2H$ -TaS₂, *J. Phys. Chem. Solids* **53**, 1259 (1992).
- [20] The experiment in Ref. [18] was done using monolayer $1T$ -TaSe₂ on $1H$ -TaSe₂. They have the same structure as $1T$ -TaS₂ and $1H$ -TaS₂. The monolayer $1T$ -TaSe₂ is also a Mott insulator, while its bulk form is a metal.
- [21] A. Ribak, R. M. Skiff, M. Mograbi, P. K. Rout, M. H. Fischer, J. Ruhman, K. Chashka, Y. Dagan, and A. Kanigel, Chiral superconductivity in the alternate stacking compound $4Hb$ -TaS₂, *Sci. Adv.* **6**, eaax9480 (2020).
- [22] A. Almoalem, I. Feldman, M. Shlafman, Y. E. Yaish, M. H. Fischer, M. Moshe, J. Ruhman, and A. Kanigel, Evidence of a two-component order parameter in $4Hb$ -TaS₂ in the Little-Parks effect, [arXiv:2208.13798](https://arxiv.org/abs/2208.13798).
- [23] I. Silber, S. Mathimalar, I. Mangel, A. K. Nayak, O. Green, N. Avraham, H. Beidenkopf, I. Feldman, A. Kanigel, A. Klein, M. Goldstein, A. Banerjee, E. Sela, and Y. Dagan, Two-component nematic superconductivity in $4Hb$ -TaS₂, *Nat. Commun.* **15**, 824 (2024).
- [24] G. Chen, Is spontaneous vortex generation in superconducting $4Hb$ -TaS₂ from vison-vortex nucleation with \mathbb{Z}_2 topological order? [arXiv:2208.03995](https://arxiv.org/abs/2208.03995).
- [25] C. Liu, S. Chatterjee, T. Scaffidi, E. Berg, and E. Altman, Magnetization amplification in the interlayer pairing superconductor $4Hb$ -TaS₂, [arXiv:2307.10389](https://arxiv.org/abs/2307.10389).
- [26] E. J. König, Type-II heavy Fermi liquids and the magnetic memory of $4Hb$ -TaS₂, *Phys. Rev. Res.* **6**, L012058 (2024).
- [27] T. Senthil, S. Sachdev, and M. Vojta, Fractionalized Fermi liquids, *Phys. Rev. Lett.* **90**, 216403 (2003).
- [28] V. Kalmeyer and R. B. Laughlin, Equivalence of the resonating-valence-bond and fractional quantum Hall states, *Phys. Rev. Lett.* **59**, 2095 (1987).
- [29] A. Szasz, J. Motruk, M. P. Zaletel, and J. E. Moore, Chiral spin liquid phase of the triangular lattice Hubbard model: A density matrix renormalization group study, *Phys. Rev. X* **10**, 021042 (2020).
- [30] T. Cookmeyer, J. Motruk, and J. E. Moore, Four-spin terms and the origin of the chiral spin liquid in Mott insulators on the triangular lattice, *Phys. Rev. Lett.* **127**, 087201 (2021).
- [31] X. G. Wen, F. Wilczek, and A. Zee, Chiral spin states and superconductivity, *Phys. Rev. B* **39**, 11413 (1989).
- [32] I. Affleck, Z. Zou, T. Hsu, and P. W. Anderson, $Su(2)$ gauge symmetry of the large- u limit of the Hubbard model, *Phys. Rev. B* **38**, 745 (1988).
- [33] X.-G. Wen, Quantum orders and symmetric spin liquids, *Phys. Rev. B* **65**, 165113 (2002).
- [34] X.-Y. Song, A. Vishwanath, and Y.-H. Zhang, Doping the chiral spin liquid: Topological superconductor or chiral metal, *Phys. Rev. B* **103**, 165138 (2021).
- [35] S. Sachdev, *Quantum Phases of Matter*, 1st ed. (Cambridge University Press, Cambridge, England, 2023).
- [36] S. Banerjee, W. Zhu, and S.-Z. Lin, Electromagnetic signatures of a chiral quantum spin liquid, *npj Quantum Mater.* **8**, 1 (2023).
- [37] Y.-F. Jiang and H.-C. Jiang, Topological superconductivity in the doped chiral spin liquid on the triangular lattice, *Phys. Rev. Lett.* **125**, 157002 (2020).
- [38] Y. Huang and D. N. Sheng, Topological chiral and nematic superconductivity by doping Mott insulators on triangular lattice, *Phys. Rev. X* **12**, 031009 (2022).
- [39] W. Wang, Y. Ou, C. Liu, Y. Wang, K. He, Q.-K. Xue, and W. Wu, Direct evidence of ferromagnetism in a quantum anomalous Hall system, *Nat. Phys.* **14**, 791 (2018).
- [40] S. Grover, M. Bocarsly, A. Uri, P. Stepanov, G. Di Battista, I. Roy, J. Xiao, A. Y. Meltzer, Y. Myasoedov, K. Pareek, K. Watanabe, T. Taniguchi, B. Yan, A. Stern, E. Berg, D. K. Efetov, and E. Zeldov, Chern mosaic and Berry-curvature magnetism in magic-angle graphene, *Nat. Phys.* **18**, 885 (2022).
- [41] O. I. Motrunich, Orbital magnetic field effects in spin liquid with spinon Fermi sea: Possible application to κ -(ET)₂Cu₂(CN)₃, *Phys. Rev. B* **73**, 155115 (2006).
- [42] L. N. Bulaevskii, C. D. Batista, M. V. Mostovoy, and D. I. Khomskii, Electronic orbital currents and polarization in Mott insulators, *Phys. Rev. B* **78**, 024402 (2008).
- [43] S. Banerjee and S.-Z. Lin, Emergent orbital magnetization in Kitaev quantum magnets, *SciPost Phys.* **14**, 127 (2023).
- [44] S. Moroz, A. Prem, V. Gurarie, and L. Radzihovsky, Topological order, symmetry, and Hall response of two-dimensional spin-singlet superconductors, *Phys. Rev. B* **95**, 014508 (2017).
- [45] T. Senthil and M. P. A. Fisher, Fractionalization in the cuprates: Detecting the topological order, *Phys. Rev. Lett.* **86**, 292 (2001).
- [46] T. H. Hsieh, Y.-M. Lu, and A. W. W. Ludwig, Topological bootstrap: Fractionalization from Kondo coupling, *Sci. Adv.* **3**, e1700729 (2017).